Fragment mass distribution of the ^{239}Pu(d,pf) reaction via the superdeformed β-vibrational resonance

K. Nishio,[1] H. Ikezoe,[1] Y. Nagame,[1] S. Mitsuoka,[1] I. Nishinaka,[1] L. Duan,[2] K. Satou,[1] S. Goto,[3] M. Asai,[1] H. Haba,[1] K. Tsukada,[1] N. Shinohara,[1] S. Ichikawa,[1] and T. Ohsawa[4]

[1]*Advanced Science Research Center, Japan Atomic Energy Research Institute, Tokai-mura, Ibaraki 319-1195, Japan*

[2]*Institute of Modern Physics, Chinese Academy of Sciences, 730000 Lanzhou, China*

[3]*Department of Chemistry, Faculty of Science, Niigata University, Niigata 950-2181, Japan*

[4]*Department of Electrical & Electronic Engineering, School of Science & Engineering, Kinki University, Osaka 577-8502, Japan*

(Received 25 June 2002; published 23 January 2003)

We measured, for the first time, the mass distribution of ^{240}Pu fission fragments following the β-vibrational resonance, whose level is formed on the second minimum of the double-humped fission barrier. The distribution shows an asymmetric mass distribution similar to the one observed for thermal neutron-induced fission of ^{239}Pu and isomeric fission of ^{240}Pu. This indicates that the ^{240}Pu system following the β-vibrational resonance descends into a fission valley which is identical to the fission valley of the ^{240}Pu isomer and ^{239}Pu$(n_{\rm th},f)$.

DOI: 10.1103/PhysRevC.67.014604 PACS number(s): 24.30.−v, 24.50.+g, 25.85.−w

I. INTRODUCTION

For excitation energies not too far above the fission barrier, the nucleus passing over the saddle point is ''cold,'' since the major part of its energy is bound in potential energy of deformation. The quantum states available to the nucleus at the saddle point, ''fission channels'' [1], represent simple collective motions similar to those of the ground state, and the system can fission through the channel whose threshold energy depends on the state. For the ^{239}Pu target capturing low energy neutrons (resonance region), the nuclear spin is limited to $J^{\pi}=0^{+}$ and $J^{\pi}=1^{+}$. The fission channel for ^{240}Pu is characterized by a quantum number as $K^{\pi}=0^{+}$ and 1^{+}, where K stands for the projection of the spin J on the symmetry axis of a fissioning nucleus. Here, the $K^{\pi}=0^{+}$ state is the ground state at the saddle, and the $K^{\pi}=1^{+}$ state can result from the combination of the two octupole vibrations of $K^{\pi}=0^{-}$ (mass asymmetry) and $K^{\pi}=1^{-}$ (bending) [2], whose threshold lies at 200 keV above the neutron binding energy [3].

For neutron-induced fission of ^{239}Pu, there is an old investigation on the mass division following the neutron capture resonance [4,5]. The results [5] show, in the abundance of ^{99}Mo and ^{115}Cd, that fission through the $J^{\pi}=1^{+}$ state enhances the relative abundance of mass-asymmetric fission products (^{99}Mo) compared to fission through the $J^{\pi}=0^{+}$ state. This was interpreted in Ref. [6] as an effect of the collective motion at the saddle point that the octupole vibration of $K^{\pi}=1^{+}$ with mirror asymmetry results in the enhanced mass asymmetry compared to the ground state of $K^{\pi}=0^{+}$, namely, the vibrational motion at the saddle point drives the system to the asymmetric fission mode (path). Supporting this interpretation, it would be natural to presume that when the β vibration with $K^{\pi}=0^{+}$ is populated at the middle stage of the fission process the resulting fission may have a symmetric fission component larger than the thermal neutron-induced fission due to vibrational motion with mirror symmetry. This collective motion cannot exist on the saddle point because the β-deformation is the major deformation parameter in the fission process and the corresponding quasistable state is not allowed. However, we can find the β-vibrational state on the second minimum of the double-humped fission barrier [superdeformed minimum: (SD)], whose structure comes from the deformation-dependent shell-correction energy [7,8] applied to the liquid-drop potential [9]. The β-vibrational state is observed below the threshold energy in the form of an enhanced fission cross section due to resonance tunneling induced when the excitation energy ($E_{\rm ex}$) of the compound nucleus matches the level [10–15].

We are interested in resonance fission through the β-vibrational state of $K^{\pi}=0^{+}$ built on the SD which has a mass symmetric shape [16]. We expect for this specific case that near-symmetric fission would be enhanced. In this paper we measured the mass distribution of fission fragments by gating on this resonance.

Our choice for this study was ^{240}Pu populated by ^{239}Pu(d,p) reaction. Plutonium-240 is one of the nuclei for which the properties of the β-vibrational state were extensively investigated. The transmission resonance at $E_{\rm ex}=5.1$ MeV has a peak of about 250-keV width [11,13]. By improving the energy resolution to measure the outgoing proton, the resonance has been resolved into intermediate structures arising from the multiple set of rotational bands with $K^{\pi}=0^{+}$ [15]. This K value was derived by measuring the fission fragment angular distribution. Direct fission without interacting levels in the second minimum at 5.1 MeV provides a minor contribution [14], so that the 5.1-MeV state works as the ''$K^{\pi}=0^{+}$ filter.'' We have determined the excitation energy of ^{240}Pu by measuring protons using silicon detectors as in Refs. [10,11]. Although the energy resolution of this method is limited to about 50 keV and cannot decompose the 5.1-MeV resonance into fine levels, our objective to select the events through the β-vibrational state will be attained.

II. EXPERIMENT

The reaction ^{239}Pu(d,pf) was used to study resonance fission of ^{240}Pu. The 13.5-MeV deuteron beam was supplied

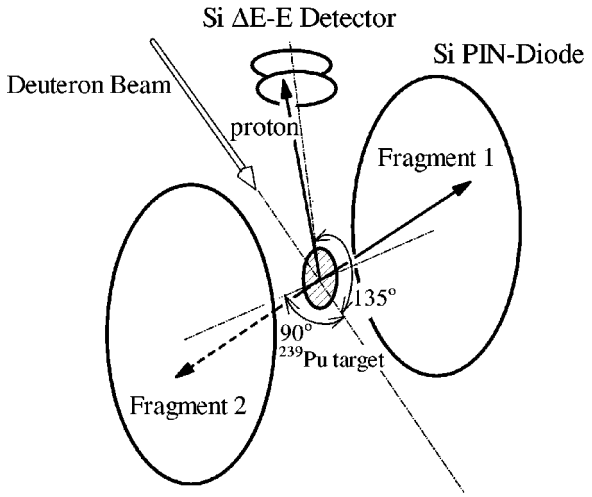

FIG. 1. Experimental setup for the fission fragment mass distribution in the ^{239}Pu(d,pf) reaction.

by the JAERI-tandem accelerator, and the typical beam current was 5 nA. The energy was changed to 12.5 and 14.5 MeV for calibration purpose.

The ^{239}Pu target was made by electrodeposition of $^{239}PuO_2(NO_3)_2$ on a 90-μg/cm^2-thick nickel foil, and the target thickness was 35 μg/cm^2. The deposition side was covered by a nickel foil with similar thickness. We also made a ^{198}Pt target to produce elastically scattered deuterons and to calibrate the proton detectors. This target was made by sputtering the enriched material on a 50-μg/cm^2 carbon foil.

The experimental setup is shown schematically in Fig. 1. The outgoing protons resulting from the (d,p) reaction were detected by a ΔE-E telescope which consisted of 300-μm (ΔE) and 1500-μm (E) thick silicon detectors. The active area of both detectors is 150 mm^2. The telescope was set at 135° relative to the beam direction with a solid angle of 45 msr. We cooled the silicon detector down to $-25\,^{\circ}$C to suppress any leakage current. The protons were easily distinguished from deuterons and tritons on the ΔE-E map, allowing the selection of neutron transfer events. The ΔE detector could be moved in the vacuum chamber so that the E detector could view the target directly. In this arrangement, the E detector was exposed to elastically scattered deuterons. By changing the beam energy to 12.5, 13.5, and 14.5 MeV, the corresponding elastic peaks were used to calibrate the E detector. The calibration of the ΔE detector was made in the ΔE-E configuration. The correspondence of energy deposition in the ΔE detector, which is given by subtracting the energy measured in the E detector from the scattering energy, to the peak channel was used to construct the calibration curve.

Two fission fragments were coincidentally detected by two silicon PIN diodes, which were equipped on both sides of the target with a similar aperture. The center of the PIN diodes were set at 90° to the beam direction. The diodes which have an active area of 1000 mm^2 each were masked by plates having a circular hole of 31.9 mm diameter, and each diode was viewed by the target at a solid angle of 1.25 sr.

The time difference between the fission signal and the proton signal was also recorded to exclude events of random coincidence. By using this information, the probability of the random events which enter in the ^{239}Pu(d,pf) fission is reduced to be 6×10^{-3}.

Data recording was triggered when two fission fragments were detected. In order to check the gain stability of the ΔE-E telescope, elastically scattered deuterons were recorded every 6–10 h.

III. DATA ANALYSIS

The energy resolution of the ΔE-E telescope was 55 keV (full width at half maximum), which was determined by the elastic peak of the deuteron. The resolution includes the energy spread of about 30 keV arising from the kinetic effect. We also made the same calibration procedure using the ^{198}Pt target. With this process, we obtained calibration constants which were almost identical to that derived using the ^{239}Pu target.

The proton energy was transformed to the excitation energy of ^{240}Pu using the mass table of Ref. [17] [the Q value for the ground state nuclear transfer in ^{239}Pu$(d,p)^{240}$Pu is 4.31 MeV].

We made the energy calibration of the silicon PIN diode by using the Schmitt formula [18]. For a fragment mass m, this formula transforms pulse height channel X to energy E as

$$E(X,m)=(a+a'm)X+b+b'm. \tag{1}$$

In general, it is difficult to determine the calibration constants (a, a', b, and b'); however, for thermal neutron-induced fission of target nuclei such as ^{233,235}U and ^{239}Pu, these constants are easily determined from the pulse height spectrum $S(X)$. In the Schmitt calibration process, by finding the midpoint channel of a line ($P_{\rm L}$ and $P_{\rm H}$) drawn between the $\frac{3}{4}$-maximum points of the light (L) and heavy (H) fragment groups, calibration constants are determined as

$$a=c_1/(P_{\rm L}-P_{\rm H}), \tag{2}$$

$$a'=c_2/(P_{\rm L}-P_{\rm H}), \tag{3}$$

$$b=d_1-aP_{\rm L}, \tag{4}$$

$$b'=d_2-a'P_{\rm H}. \tag{5}$$

The parameters, c_1, c_2, d_1, and d_2, depend on the target nucleus.

In our measurement we observed the compound nucleus ^{240}Pu also at excitation energies $E_{\rm ex}$ close to excitation energies after thermal neutron-induced fission of ^{239}Pu ($E_{\rm ex}=6.53$ MeV). This tells that by constructing the spectrum $S(X)$ using events around $E_{\rm ex}=6.53$ MeV, the Schmitt calibration procedure can be adopted in the ^{239}Pu(d,pf) measurement. Figure 2 shows the pulse height spectrum for ^{239}Pu(d,pf), obtained by selecting the events in $6.0<E_{\rm ex}<7.0$ MeV. The solid curve in this figure is the result of decomposing the experimental data to two Gaussian distri-

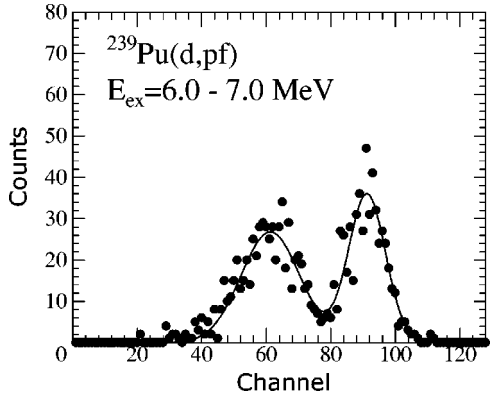

FIG. 2. Pulse height spectrum $S(X)$ of fission fragment obtained in the silicon PIN diode. Curve is the result of the fitting of the spectrum to two Gaussian distributions with equal areas.

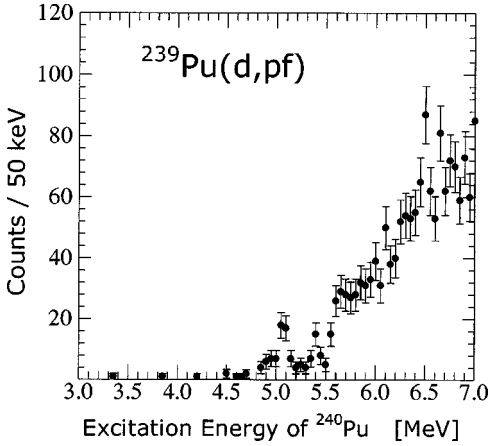

FIG. 3. Number of coincidence events between fission fragments and proton plotted as a function of excitation energy of ^{240}Pu.

butions having the same area. The centroid of two Gaussian components obtained in the fitting process were used as P_{L} and P_{H}. This calibration procedure does not show significant differences to the one based on the midpoint of $\frac{3}{4}$-maximum level line for the present case which has a rather large statistical error. Then, we obtained the calibration constants in Eqs. (2)–(5) by using parameters $(c_1,\ c_2,\ d_1,\ d_2)$ $=(27.6654,\ 0.041\,06,\ 89.0064,\ 0.1362)$ [19], reported in the $^{239}\mathrm{Pu}(n_{\mathrm{th}},f)$ study.

Fission fragment masses m_1 and m_2 were determined from the pulse height of both fragments X_1 and X_2 by following the mass and momentum conservation law. An iteration procedure was used to numerically determine the mass number of the fission fragment. In this analysis, we determined the primary fragment mass, i.e., mass before neutron evaporation. This needs a number of neutron emission as a function of fragment mass $\nu(m)$, for which data of Tsuchiya *et al.* [20] were used. These $\nu(m)$ data agree with those measured in Ref. [21] within 20% in every mass region.

IV. EXPERIMENTAL RESULTS AND DISCUSSION

Figure 3 shows the proton-fission coincidence events plotted as a function of excitation energy of ^{240}Pu. This spectrum was obtained under a condition on the time difference between the fission detector and the proton detector in order to supress random coincidences. The energy bin is set at 50 keV corresponding to the present resolution. The resonance peak is observed at 5.05 MeV. For excitation energies below the neutron binding energy (6.53 MeV), where neutron emission is energetically hindered and the γ-ray emission is the only decay mode competing with fission in the decay channel, the spectrum in Fig. 3 is related to the ''fission probability'' multiplied by the ''population probability'' of the compound nucleus in the transfer reaction $^{239}\mathrm{Pu}(d,p)^{240}\mathrm{Pu}$. The resonance energy of 5.05 MeV obtained in this work is close to that measured by Glässel *et al.* [14] and Hunyadi *et al.* [15].

By measuring the $^{239}\mathrm{Pu}(d,pf)$ reaction, fission events resulting from excitation energies near the first fission barrier height ($E_{\mathrm{A}}=5.80$ MeV [12]) could be obtained. We show first in Fig. 4(A) the mass yield curve following the excited compound nucleus of $6.0\geqslant E_{\mathrm{ex}}>5.3$ MeV. The yield is normalized such that the sum of the yields becomes 200%. The mass bin is set at 2.0 amu to gain statistics. This spectrum agrees with that for thermal neutron-induced fission of ^{239}Pu [22] ($E_{\mathrm{ex}}=6.53$ MeV) shown by the solid curve. The data of Ref. [22] were obtained by measuring the kinetic energies of both fragments ($2E$ method) by using silicon detectors similar to our experimental method.

Fission events through the vibrational resonance being characterized by their excitation energy between $4.78<E_{\mathrm{ex}}$ $\leqslant 5.30$ MeV (see Fig. 3) result in the mass yield in Fig. 4(B). We set the mass bin as 5 amu. Although the mass yield curve constructed by using only about 80 events has a large uncertainty, the asymmetric fission character is evident, and the yield agrees with that for $^{239}\mathrm{Pu}(n_{\mathrm{th}},f)$ as well as the gross trend that the sharp rise in the near symmetric region when going from the heavy fragment mass $m_{\mathrm{H}}=125$–135 amu and the gradual decrease in the far asymmetric region from m_{H} $=140$–160 amu. The yield reaches the maximum at m_{H} ~ 135 amu for all spectra shown in Fig. 4. We have determined the average value of the heavy fragment mass as $\langle m_{\mathrm{H}}\rangle=140.2\pm 2.8$ amu, where the error comes from the binning and the uncertainty arising from the energy calibration process. This agrees with the value 139.8 ± 1.1 amu obtained from the spectra in Fig. 4(A) within the error and with the value 139.7 amu for $^{239}\mathrm{Pu}(n_{\mathrm{th}},f)$ [22]. The present data then lead to the conclusion that fission through the β-vibrational resonance does not show any significant enhancement in the symmetric mass division within the error.

The fission fragment mass resolution affects the standard deviation (σ_{m}) of the mass distribution for the heavy (or light) fragment group and the peak to valley ratio (P/V); i.e., the maximum yield divided by the symmetric fission yield. These quantities can be compared to the well known mass distribution of $^{239}\mathrm{Pu}(n_{\mathrm{th}},f)$ to find the present mass resolution. By gating on the excitation energy in the interval of $6.0<E_{\mathrm{ex}}<7.0$ MeV and constructing the corresponding mass yield curve, we obtained $\sigma_{\mathrm{m}}=7.2$ amu and P/V $=35^{+35}_{-10}$. Note that the average excitation energy in these

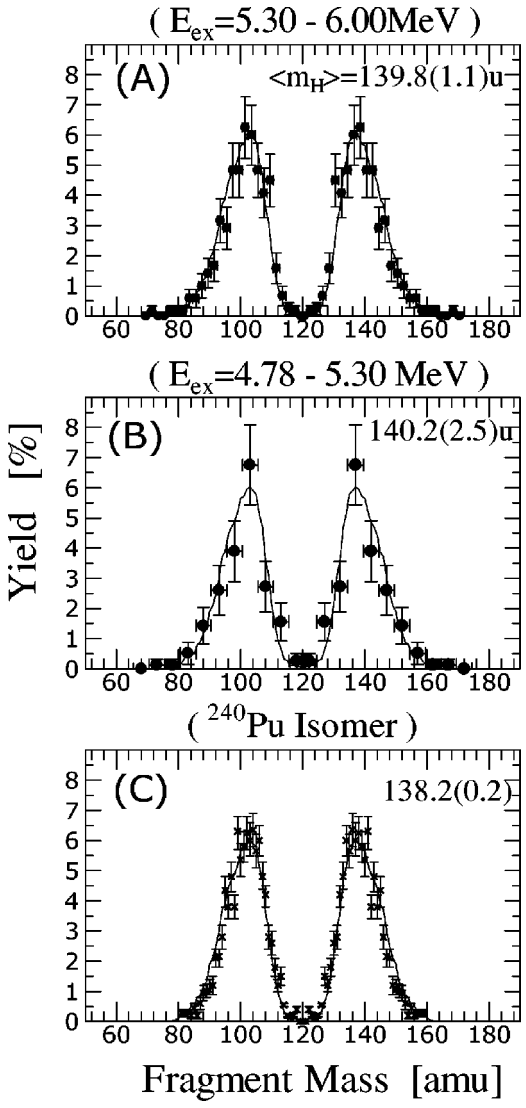

FIG. 4. Mass yield curves obtained for the ^{239}Pu(d,pf) reaction, (A) and (B). These spectra are made by setting the excitation energy range as (A) $6.0 \geqslant E_{ex} > 5.3$ MeV and (B) $5.30 \geqslant E_{ex} > 4.78$ MeV. The average value for the heavy fragment mass $\langle m_H \rangle$ is shown in each section of the figure. The error shown in (A) and (B) comes from the binning and the uncertainty arising from the energy calibration process. Mass yield curve for the isomer fission [23] is shown in (C). Solid curve appearing in the every section is the data for ^{239}Pu(n_{th},f) [22].

events was 6.55 MeV and almost agreed with 6.53 MeV for ^{239}Pu(n_{th},f). The ^{239}Pu(n_{th},f) data in Ref. [22] reported $\sigma_m = 6.64$ and $P/V = 114 \pm 2$. When the mass yield curve in Ref. [22] is broadened with standard deviation $\sigma = 2.8$ amu ($\sqrt{7.2^2 - 6.64^2}$), the P/V value of the broadened spectrum agreed with that obtained in this measurement.

We want to show in Fig. 4(C) the mass yield for the fission of shape isomer in ^{240}Pu [23] (half-life is 3.8 ns [24]). This is localized in the SD of the double-humped fission barrier (2.25 MeV above the ground state) [15], and has the (J^π,K) value of $(0^+,0)$. Isomeric fission forms a good reference in the sense that the nuclear shape is the same as that experienced by the β-vibirational fission. Isomeric fission forms a mass distribution similar to that for ^{239}Pu(n_{th},f) and hence to the β-vibrational fission in Fig. 4(B).

Regier *et al.* [4] found in their radiochemical experiment of determining the ratio of the yield of ^{99}Mo to ^{115}Cd, R, that fission through the $E_n = 0.3$ eV ($J^\pi = 1^+$) resonance has a three times larger R value than ^{239}Pu(n_{th},f). This may suggest that fission through the $J^\pi = 1^+$ state has a larger mass asymmetry than the 0^+ state, based on the consideration that ^{239}Pu(n_{th},f) fission originates from the mixed states of $J^\pi = 1^+$ and 0^+. The relative abundance of the former and the latter spin state leading to fission are 37.2% and 62.8°, respectively, determined on the basis of the Reich-Moore formula [25] to calculate the neutron induced fission cross section and the resonance parameters compiled in JENDL-3.2 [26].

The recent work by Hambsch *et al.* [27], however, should be mentioned. They measured the fragment mass distribution for the neutron capture resonances of ^{239}Pu with the $2E$ method using the double Frisch-gridded ionization chamber. They show the ratio of the mass yield at the 0.3-eV resonance to that of thermal neutron-induced fission, $Y_{0.3}(m)/Y_{th}(m)$. At the region around $m = 99$ amu, the $Y_{0.3}/Y_{th}$ is almost 1.0, and the $m = 115$-amu region has 0.85 ± 0.10. This results in the $R_{0.3}/R_{th}$ value of 1.18 ± 0.14, showing a weak variation in the R value. This contradicts the value 3.00 ± 0.28 that Regier *et al.* have obtained. The reason for the different results in these measurements is not clear except for the experimental methods they have adopted. If discussion is allowed to continue based on the results of the $2E$ method we have adopted, the agreement of the mass yield between the isomeric fission and the thermal neutron-induced fission suggests that the ^{239}Pu(n_{th},f) reaction is characterized as following the $(J^\pi,K) = (0^+,0)$ state at the saddle point in the limit of fragment mass formation. This is supported by the dominance of the $J^\pi = 0^+$ fission for ^{239}Pu(n_{th},f) (62.8%).

The relative fission cross section $\alpha(J^\pi)$ from the state J^π in the β-vibrational levels ($K^\pi = 0^+$) on the SD was investigated by Hunyadi *et al.* [15], who could fit the structure of the fission cross section at the 5.1-MeV resonance by using $\alpha(0^+) = 0.19$, $\alpha(2^+) = 0.66$, and $\alpha(4^+) = 0.15$, showing the dominance of the nonzero spin J fissions (81%). The similar mass distribution for the thermal neutron-induced fission, isomeric fission and the β-vibrational fission suggests that a difference in spin of $J = 2$ or 4 introduced into the system does not cause a significant change in the resulting mass distribution.

In fission of the ^{240}Pu isomer, the second barrier and the following valley structure on the potential energy surface play a role in determining the fragment mass distribution. As is suggested in the calculation in Ref. [28], the fission path of the system bifurcates into mass symmetric and asymmetric valleys beyond the deformation of the second minimum. The lowering of the second fission barrier for the asymmetric deformation dominates the barrier penetration and forces the system to fall in the asymmetric potential valley, explaining the asymmetric mass distribution for the isomeric ^{240}Pu fission. For resonance fission through the β-vibrational states

on the SD, the system should end up in the asymmetric potential valley into which the isomeric ^{240}Pu system descends.

V. SUMMARY

Motivated by the speculation that the β vibration on the SD of the double-humped fission barrier would result in an enhancement of the symmetric mass components, the mass distribution of ^{240}Pu following the resonance tunneling originating from this level was measured for the first time. The obtained distribution shows an asymmetric mass division similar to the one for the thermal neutron-induced fission of ^{239}Pu and the isomeric fission of ^{240}Pu. This indicates that the system through β-vibrational resonance comes out in the asymmetric fission valley that the ^{240}Pu isomer and ^{239}Pu(n_{th},f) descend.

ACKNOWLEDGMENTS

The authors thank the crew of the JAERI-tandem facility for the beam operation. Special thanks are due to Dr. T. Nakagawa of Nuclear Data Center in JAERI for the calculation of thermal neutron-induced fission cross section from the $J^{\pi}=0^{+}$ and 1^{+} states. We thank Professor Y. Nakagome of Kyoto University for fruitful discussions. The present study was supported by the REIMEI Research Resources of Japan Atomic Energy Research Institute.

[1] A. Bohr, *Proceedings of the International Conference on Peaceful Use of Atomic Energy*, Geneva, 1955 (United Nations, New York, 1956), Vol. II, p. 151.
[2] J.J. Griffin, *Proceedings of the IAEA Symposium on Physics and Chemistry of Fission*, Salzburg (IAEA, Vienna, 1965), Vol. I, p. 23.
[3] H. Derrien, G. de Saussure, and R. B. Perez, Nucl. Sci. Eng. **106**, 434 (1990).
[4] R.B. Regier, W.H. Burgus, R.L. Tromp, and B.H. Sorensen, Phys. Rev. **119**, 2017 (1960).
[5] G.A. Cowan, B.P. Bayhurst, R.J. Prestwood, J.S. Gilmore, and G.W. Knobeloch, Phys. Rev. **144**, 979 (1966).
[6] A. Michaudon, *Advances in Nuclear Physics* (Plenum Press, New York, 1973), Vol. 6, p. 1.
[7] V. M. Strutinsky, Nucl. Phys. **A95**, 420 (1967).
[8] S. Bjønholm and J.E. Lynn, Rev. Mod. Phys. **52**, 725 (1980).
[9] D.L. Hill and J.A. Wheeler, Phys. Rev. **89**, 1102 (1953).
[10] B.B. Back, J.P. Bondorf, G.A. Otroshenko, J. Pedersen, and B. Rasmussen, *Proceedings of the IAEA Symposium on Physics and Chemistry of Fission*, Vienna (IAEA, Vienna, 1969), p. 351.
[11] B.B. Back, J. Bondorf, G. Otroschenko, J. Pederson, and B. Rasmussen, Nucl. Phys. **A165**, 449 (1971).
[12] B.B. Back, O. Hansen, H.C. Britt, and J.D. Garrett, Phys. Rev. C **9**, 1924 (1974).
[13] H.J. Specht, J.S. Fraser, J.C.D. Milton, and W.G. Davies, *Proceedings of the IAEA Symposium in Physics and Chemistry of Fission*, Vienna (IAEA, Vienna, 1969), p. 363.
[14] P. Glässel, H. Rösler, and H.J. Specht, Nucl. Phys. **A256**, 220 (1976).
[15] M. Hunyadi, D. Gassmann, A. Krasznahorkay, D. Habs, P.G. Thirolf, M. Csatlos, Y. Eisermann, T. Faestermann, G. Graw, J. Gulyas, R. Hertenberger, H.J. Maier, Z. Mate, A. Metz, and M.J. Chromik, Phys. Lett. B **505**, 27 (2001).
[16] Mass symmetry at the second minimum (SD) is predicted in the calculation of the potential energy surface as seen in P.A. Butler and W. Nazarewicz, Rev. Mod. Phys. **68**, 349 (1996).
[17] G. Audi and A.H. Wapstra, Nucl. Phys. **A595**, 409 (1995).
[18] H.W. Schmitt, W.M. Gibson, J.H. Neiler, F.J. Walter, and T.D. Thomas, *Proceedings of the Symposium on Physics and Chemistry of Fission*, Salzburg (IAEA, Vienna, 1965), Vol. 1, p. 531.
[19] J.N. Neiler, F.J. Walter, and H.W. Schmitt, Phys. Rev. **149**, 894 (1966).
[20] C. Tsuchiya, Y. Nakagome, H. Yamana, H. Moriyama, K. Nishio, I. Kanno, K. Shin, and I. Kimura, J. Nucl. Sci. Technol. **37**, 941 (2000).
[21] V.F. Apalin, Yu.N. Gritsyuk, I.E. Kutikov, V.I. Lebedev, and L.A. Mikaelian, Nucl. Phys. **71**, 553 (1965).
[22] C. Wagemans, E. Allaert, A. Deruytter, R. Barthélémy, and P. Schillebeeckx, Phys. Rev. C **30**, 218 (1984).
[23] J. Weber, H.J. Specht, E. Konecny, and D. Heunemann, Nucl. Phys. **A221**, 414 (1974).
[24] H.C. Britt, B.H. Erkkila, and B.B. Back, Phys. Rev. C **6**, 1090 (1972).
[25] H. Derrien, G. de Saussure, and R.B. Perez, Nucl. Sci. Eng. **106**, 434 (1990); H. Derrien, J. Nucl. Sci. Technol. **30**, 845 (1993); C.W. Reich and M.S. Moore, Phys. Rev. **111**, 929 (1958).
[26] T. Nakagawa, K. Shibata, S. Chiba, T. Fukahori, Y. Nakajima, Y. Kikuchi, T. Kawano, Y. Kanda, T. Ohsawa, H. Matsunobu, M. Kawai, A. Zukeran, T. Watanabe, S. Igarasi, K. Kosako, and T. Asami, J. Nucl. Sci. Technol. **32**, 1259 (1995).
[27] F.-J. Hambsch, L. Dematté, H. Bax, and I. Ruskov, J. Nucl. Sci. Technol. **2**, 307 (2002).
[28] P. Möller and J.R. Nix, *Proceedings of the Symposium on Physics and Chemistry of Fission*, Rochester (IAEA, Vinenna, 1973), Vol. 1, p. 103.